SOME THEORETICAL CONSIDERATIONS ON REMOTE PROBING OF WEAKLY SCATTERING IRREGULARITIES

By B. H. BRIGGS* and R. A. VINCENT*

[Manuscript received 11 April 1973]

Abstract

A basis is presented for the interpretation of electromagnetic or acoustic remote probing experiments in which back-scattering from horizontally stratified atmospheric irregularities is observed by radar techniques. The treatment takes into account geometrical factors and the polar diagrams of the transmitter and receiver. It is shown that single frequency observations give no information about the form of the irregularities if they are isotropic but that, if they are anisotropic with different horizontal and vertical scales, information about their horizontal scales may be obtained in some cases. The range of validity of some approximations introduced is tested by exact numerical computation for a typical example.

I. INTRODUCTION

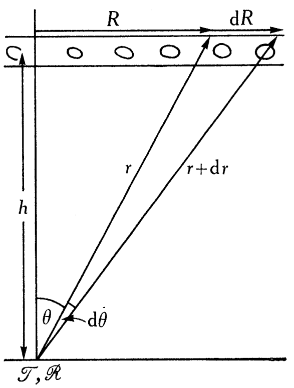

Fig. 1.—Remote probing situation in which irregularities at height h are observed by means of waves back-scattered from transmitter $\mathscr{T}$ to receiver $\mathscr{R}$.

A number of remote probing experiments performed on the atmosphere have been based on the experimental arrangement illustrated in Figure 1. A point source transmitter $\mathscr{T}$, usually operating in the pulsed mode, is situated relatively close to the horizontally stratified irregularities, and the back-scattered echoes from the irregularities are observed with a receiver $\mathscr{R}$ situated close to the transmitter. For example, this method was used by Gardner and Pawsey (1953) to observe partial reflections from the D-region of the ionosphere using radio waves, and by McAllister *et al.* (1969) to observe structure in the troposphere using sound waves (acoustic sounding). The objectives of such experiments are to obtain information about the occurrence, strength, scale, shape, and movement of the irregularities. To this end, spaced receivers have often been used to determine the correlation of the scattered wave field at different points on the ground, and various theoretical techniques have been developed to derive the variation of returned power $W(\theta)$ as a function of the off-vertical angle θ. Clearly a theory is required to relate such observations to the physical properties of the irregularities.

Characteristic features of these experiments that need to be taken into account by a theoretical explanation are: the transmitter and receiver each have separate polar diagrams $\mathscr{T}(\theta)$ and $\mathscr{R}(\theta)$, which affect the variation of received power as a function of the off-vertical angle; signals scattered from large off-vertical angles

* Department of Physics, University of Adelaide, Adelaide, S.A. 5001.

come from a greater range and therefore undergo greater distance attenuation; and the scattering properties of the irregularities themselves. Furthermore, if the horizontal scale of the irregularities is large, the assumption of plane wave illumination of the irregularities may not be valid, and the curvature of the wavefront incident on the irregularity may have to be taken into account.

Despite the many papers dealing with the theory of scattering by irregular media, there appear to be none which take the abovementioned factors into account, and so the existing theories are not directly applicable to the experimental situation under consideration. It is the object of the present paper to provide a theoretical basis for interpreting such experiments. Although we restrict our theory to the case of back-scattering with the transmitter and receiver close together, the treatment is kept as general as possible, and the method presented here can be readily extended to the bistatic case in which the transmitter and receiver are separated. Specific applications to the observation of *D*-region partial reflections are considered in the following paper (Vincent 1973, present issue pp. 815–27).

An irregular scattering medium can be characterized by a function $f(x,y,z)$ which describes the scattering density at each point in the medium. We assume that the scattering is weak, so that the incident wave is not appreciably attenuated and the Born approximation can be used. If the amplitude of the incident wave at a point (x,y,z) in the medium is $A(x,y,z)$ then the amplitude of the wave isotropically scattered from the small volume element $\mathrm{d}x\,\mathrm{d}y\,\mathrm{d}z$ at this point is

$$A(x,y,z)\,f(x,y,z)\,\mathrm{d}x\,\mathrm{d}y\,\mathrm{d}z\,.$$

The statistical properties of the medium can be specified by means of the three-dimensional autocorrelation function ρ of f, defined by

$$\rho(\xi,\eta,\zeta) = \frac{\langle f(x,y,z)\,f(x+\xi,y+\eta,z+\zeta)\rangle - \langle f(x,y,z)\rangle^2}{\langle f^2(x,y,z)\rangle - \langle f(x,y,z)\rangle^2}\,.$$

Spatial scales can be defined in terms of the values of (ξ,η,ζ) at which $\rho(\xi,\eta,\zeta)$ falls to some specified value such as $0\cdot5$ or e^{-1}. The medium may not necessarily be isotropic and the scale may differ in different directions. In the atmosphere, the scale of the irregularities may be different in the vertical and horizontal directions.

It is often convenient to consider an irregular scattering medium as a superposition of individual scattering irregularities of a characteristic shape. The justification for this is the theorem (Ratcliffe 1956): if a number of similar scattering irregularities are superimposed in random positions then the autocorrelation function $\rho(\xi,\eta,\zeta)$ for the medium as a whole is the same as that for a single irregularity. Thus, for example, the angular distributions of returned power scattered by the medium and by a single irregularity of characteristic shape are identical apart from magnitude. The number of irregularities per unit volume affects only the magnitude of the total power returned. It does not matter from the point of view of this theorem whether some of the irregularities overlap others, provided that they are all in random positions.

Our method consists in calculating the scattering polar diagram of a single irregularity of a particular assumed form, and then considering an assembly of such irregularities which, together with the geometrical and polar diagram factors already mentioned, determine the resultant angular distribution of returned power. An advantage of this approach is that it is readily applied to experiments which appear to reveal the presence of single, more or less isolated, scattering clouds or irregularities. Having found the angular distribution of the received energy, the autocorrelation function of the wave field is then determined as the two-dimensional Fourier transform of this distribution. In all cases considered here, the distribution of scattered energy is symmetrical about the vertical and is therefore a function of a single variable $s = \sin\theta$. For this case, the Fourier transform becomes a Fourier–Bessel transform (Ratcliffe 1956) and the required autocorrelation function of the wave field is given by

$$\rho(\alpha') = 2\pi K_0 \int_0^\infty W(s)\,\mathrm{J}_0(2\pi\alpha' s)\,s\,\mathrm{d}s\,, \tag{1}$$

where $\rho(\alpha')$ is the complex correlation between the fields measured at points in a plane parallel to the irregularities and separated by a distance α' measured in units of the wavelength, K_0 is a constant chosen such that $\rho(0)$ is unity, and J_0 is the Bessel function of zero order. The correlation is evaluated as a time average and not as a space average (Briggs 1961). The function $\rho(\alpha')$ is a real function because of the assumed symmetry of $W(s)$ about the vertical. Assuming that the scattered components are randomly phased and that there is no superimposed specular component, the autocorrelation function $\rho_{\mathrm{A}}(\alpha')$ for the *amplitude A* of the wave field is (Ratcliffe 1956)

$$\rho_{\mathrm{A}}(\alpha') = \{\rho(\alpha')\}^2\,. \tag{2}$$

The autocorrelation function for amplitude can easily be measured experimentally by using spaced receivers.

In Section II we consider the angular distribution of returned power for the case of irregularities which are on the average spherical, so that $\rho(\xi,\eta,\zeta)$ is a function only of $\alpha = (\xi^2+\eta^2+\zeta^2)^{\frac{1}{2}}$. No matter what functional form may be assumed for $\rho(\alpha)$ it is clear that such irregularities must back-scatter in the same way at all angles of incidence and that the observed angular variation of received power depends only on distance factors and the polar diagrams of the transmitter and receiver. Consequently, observations of spherical irregularities give no information about the scale of the irregularities. In Section III we consider scattering by irregularities with different horizontal and vertical scales. In this case the resultant angular distribution of received power depends on the form of the irregularities and, for a given wavelength, the power is greatest for irregularities with a particular vertical scale. Finally, in Section IV, we investigate the range of validity of the theory by considering at what value of horizontal scale the curvature of the incident wavefront across a single irregularity becomes important.

II. Isotropic Irregularities

(*a*) *Angular Distribution of Returned Energy*

Consider the thin horizontal layer of irregularities at a mean height h that is shown in Figure 1. If the irregularities are on the average spherical, the cross section for back-scattering cannot depend upon the angle of incidence of the wave on the irregularity. This case corresponds to a medium which is statistically isotropic.

The total energy returned to the receiver at off-vertical angles between θ and $\theta+\mathrm{d}\theta$ comes from the annular ring $\mathrm{d}R$ (Fig. 1) of area $2\pi R\,\mathrm{d}R$. Let the transmitter have a power polar diagram $\mathscr{T}(\theta)$ that is assumed to be symmetrical about the vertical. Then, neglecting absorption in the medium itself, the power flux falling on the annular ring $\mathrm{d}R$ is proportional to $r^{-2}\mathscr{T}(\theta)$. Each irregularity scatters a spherical wave whose amplitude decreases as r^{-1}. Since the irregularities are in random positions, the phases at the receiver are also random and consequently the received scattered powers add. (We assume that the pulse length is sufficiently long for all returns to overlap at some point in time, and calculate the power at this time.) Thus the returned power flux in the range θ to $\theta+\mathrm{d}\theta$ is proportional to the number of irregularities, i.e. to the area of the annulus. Consequently the power flux W actually received by a receiver with power polar diagram $\mathscr{R}(\theta)$ is

$$W(\theta)\,\mathrm{d}\theta \propto r^{-4}\mathscr{T}(\theta)\mathscr{R}(\theta)\,2\pi R\,\mathrm{d}R\,.$$

We now express R and r in terms of θ via the geometric equations

$$R = h\tan\theta\,,\qquad \mathrm{d}R = h\sec^2\theta\,\mathrm{d}\theta\,,\qquad r = h\sec\theta\,,$$

and obtain

$$W(\theta)\,\mathrm{d}\theta \propto h^{-2}\mathscr{T}(\theta)\mathscr{R}(\theta)\sin\theta\cos\theta\,\mathrm{d}\theta\,. \tag{3}$$

At this point, it is interesting to note that $W(\theta)$ vanishes for $\theta = 0$, which at first sight suggests that no power is returned from directly overhead. However, the expression (3) gives the power for angles between θ and $\theta+\mathrm{d}\theta$, and not the power per unit solid angle. The element of solid angle $\mathrm{d}\Omega$ is given by

$$\mathrm{d}\Omega = 2\pi\sin\theta\,\mathrm{d}\theta$$

and so

$$W(\theta)\,\mathrm{d}\Omega \propto h^{-2}\mathscr{T}(\theta)\mathscr{R}(\theta)\cos\theta\,\mathrm{d}\Omega\,, \tag{4}$$

which has a maximum at $\theta = 0$, as would be expected on physical grounds.

(*b*) *Autocorrelation Function of Wave Field*

The autocorrelation function of the wave field in a plane parallel to the irregularities can be found immediately from the Fourier–Bessel transform of equation (1). To illustrate the method of calculation, we consider the case in which the power polar diagrams of the transmitter and receiver can each be approximated by a Gaussian function $\exp(-s^2/s_0^2)$ characterized by a single parameter s_0 determining its width. Although such polar diagrams may not be realistic their use does provide a convenient analytic check on any numerical evaluations of equation (1). In the case of Gaussian polar diagrams we have

$$\rho(\alpha') = \int_0^\infty \exp(-2s^2/s_0^2)\,s^2\,\mathrm{J}_0(2\pi\alpha' s)\,\mathrm{d}s\,, \tag{5}$$

which is an integral of the general form

$$\int_0^\infty \exp(-a^2t^2)\,t^{\mu-1}\,\mathrm{J}_\nu(bt)\,\mathrm{d}t$$

that has the value

$$\{\Gamma(\tfrac{1}{2}\nu+\tfrac{1}{2}\mu)(\tfrac{1}{2}b/a)^{\nu}/2a^{\mu}\Gamma(\nu+1)\}\,\mathrm{M}(\tfrac{1}{2}\nu+\tfrac{1}{2}\mu,\nu+1,-\tfrac{1}{4}b^2/a^2), \tag{6}$$

where M is the confluent hypergeometric function. For the integral (5), we have $\mu = 3$, $\nu = 0$, $a^2 = 2/s_0^2$, and $b = 2\pi\alpha'$, so that the required solution is

$$\begin{aligned}\rho(\alpha') &= \tfrac{1}{4}s_0^2\,\Gamma(\tfrac{3}{2})\,\mathrm{M}(\tfrac{3}{2},1,-(\pi\alpha' s_0/\sqrt{2})^2)\\ &= 0\cdot 2215\,s_0^2\exp(-\pi\alpha' s_0/\sqrt{2})^2\,\mathrm{M}(-\tfrac{1}{2},1,(\pi\alpha' s_0/\sqrt{2})^2).\end{aligned} \tag{7}$$

As values of M are tabulated, it is a simple matter to compute $\rho(\alpha')$ for any value of s_0. Plots of $\rho(\alpha')$ for values of s_0 corresponding to angles of 10°, 20°, and 30° are shown in Figure 2. These curves have been normalized to unity at the origin.

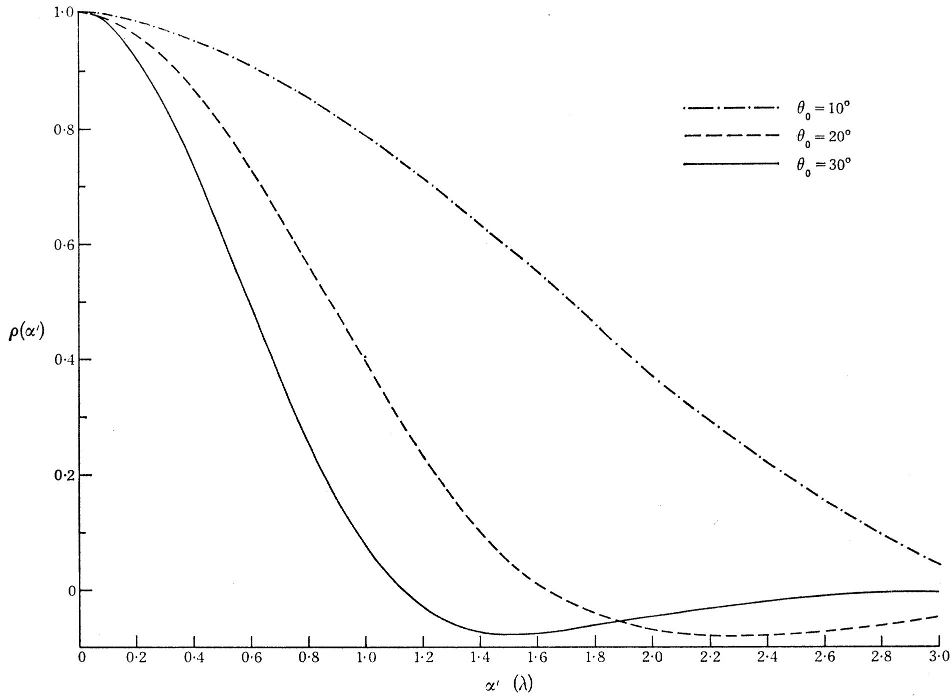

Fig. 2.—Complex correlation $\rho(\alpha')$ between fluctuations recorded by two receivers separated by a distance α'. It is assumed that the irregularities are isotropic and that the power polar diagrams of both the transmitter and receiver are Gaussians with width parameter $\sin\theta_0$.

It has been our object in this Section to emphasize that the angular distribution of received power and the scale of the pattern are independent of the size of the irregularities and the form of the radial variation of scattering density when the irregularities are isotropic. Consequently, no information about the irregularities can be obtained from measurements of the angular distribution of scattered power or of the correlation between the field variations at spaced receivers. Of course, the scale of the irregularities relative to the wavelength employed, the functional form of the radial variation, and the number of irregularities per unit volume do affect the *magnitude* of the total back-scattered power.

III. Anisotropic Irregularities

In the case of D-region partial reflections, the angular distribution of received energy is sometimes quite narrow (of the order of a few degrees) and this suggests that the scattering irregularities may have larger horizontal than vertical dimensions. We assume that there is no anisotropy in the horizontal plane, so that an individual irregularity has, on the average, symmetry about the vertical direction. The simplest mathematical approach is to assume that the anisotropy arises from a vertical compression of the isotropic irregularities which transforms the contours of constant scattering density from spheres to ellipsoids of revolution. Of the many possible radial distributions of scattering power, that which is Gaussian is considered here. Thus the scattering density distribution of a single characteristic irregularity is given by

$$f(x,y,z) \propto \exp(-x^2/a^2 - y^2/a^2 - z^2/b^2), \tag{8}$$

where the z axis is vertical and the x and y axes are horizontal. The axial ratio of the irregularity a/b is such that $a > b$, so that the irregularities have the form of horizontally flattened discs.

The three-dimensional autocorrelation function of such an irregularity is given by

$$\rho(\xi,\eta,\zeta) = \exp(-\tfrac{1}{2}x^2/a^2 - \tfrac{1}{2}y^2/a^2 - \tfrac{1}{2}z^2/b^2) \tag{9}$$

and this is also the autocorrelation function of the random medium produced by superposition of a large number of such irregularities in random positions. The horizontal scale (to e^{-1}) is therefore $\sqrt{2}\,a$ and the vertical scale $\sqrt{2}\,b$.

Reference to Figure 1 shows that irregularities in different horizontal positions are illuminated by the incident wave at different angles to the vertical axis. We therefore need an expression for the energy back-scattered as a function of the angle of incidence of the wave on the irregularity. This is easily found by first calculating the three-dimensional Fourier transform of the function (8), and then taking its value at a distance $2\lambda^{-1}$ from the origin in reciprocal space (Ratcliffe 1956). It should be noted, however, that the use of reciprocal space (as is commonly done in X-ray crystallography) requires the incident wave to be plane and the observations to be made at a large distance (the limitations imposed by these assumptions are considered in Section IV). For the moment we adopt this method as a useful approximation and obtain for the back-scattered power a factor proportional to

$$\exp(-8\pi^2\lambda^{-2}(a^2\sin^2\theta + b^2\cos^2\theta)), \qquad \text{or} \qquad \exp(-8\pi^2\lambda^{-2}\{b^2 + (a^2-b^2)s^2\}), \tag{10}$$

where λ is the wavelength of the radiation and $s = \sin\theta$. The factor (10) must now be included in equation (3) which becomes

$$W(s)\,ds \propto \exp(-8\pi^2\lambda^{-2}\{b^2 + (a^2-b^2)s^2\})\mathscr{T}(s)\mathscr{R}(s)\,s\,ds, \tag{11}$$

where the polar diagrams are expressed as functions of s rather than θ. It should be noted that, for spherical irregularities, $a = b$ and the proportionality (11) reduces to equation (3) as expected.

Once $W(s)\,\mathrm{d}s$ is known, the autocorrelation function $\rho(\alpha')$ can be found by taking a Fourier–Bessel transform as before. Owing to the large number of parameters, numerical examples are not given here (although examples involving realistic aerial polar diagrams are given in the subsequent paper (Vincent 1973)). However, it is of interest to examine the form of the function (10) for the case of a single irregularity that is approximately overhead. The back-scattered energy is then proportional to

$$\{a^2 b \exp(-4\pi^2 b^2/\lambda^2)\}^2\,, \tag{12}$$

which is plotted in Figure 3 as a function of b for a fixed value of the axial ratio a/b. It can be seen that the back-scattered energy shows a sharp peak, or resonance, for a value of $b \approx 0\cdot2\,\lambda$. This is the analogue of the well-known result that only Fourier

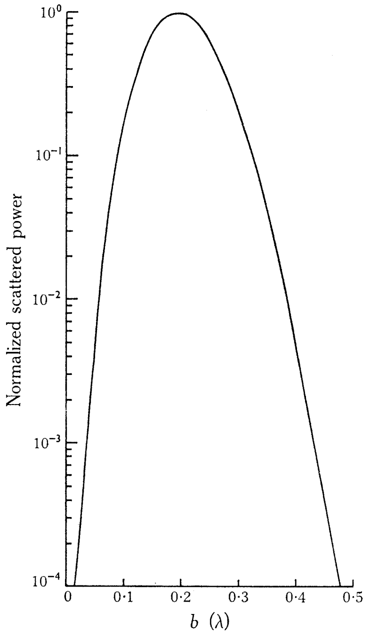

Fig. 3.—Normalized scattered power for an overhead irregularity of Gaussian form as a function of the vertical scale parameter b measured in wavelengths λ. The sharp resonance centred on $b \approx 0\cdot2\,\lambda$ indicates that irregularities of this vertical scale are preferentially selected by a probing wave of wavelength λ.

components of vertical wavelength $\frac{1}{2}\lambda$ contribute to the back-scattered energy for an incident wavelength λ. The resonance is sufficiently sharp that it is reasonable in particular instances to assume that only irregularities with $b \approx 0\cdot2\,\lambda$ are important. Certainly, if the irregularities have a range of b values but have approximately equal total scattering powers, those with $b \approx 0\cdot2\,\lambda$ dominate the observed back-scatter for a wavelength λ. Consequently, it is useful to consider the case in which $b = 0\cdot2\,\lambda$ and only a is regarded as a variable. If the polar diagrams of the transmitter and receiver are known, the angular distribution of the received power can be computed from equation (11) for various values of a, and $\rho(\alpha')$ may then be found for various values of a. Experimental observations of either the angular distribution or the correlation between spaced receivers can then be used to yield the value of a which best fits the observations.

In the case of partial reflections from the D-region, quite large values of a are required in some cases, and this raises the question of the range of validity of the present treatment. If a is so large that the curvature of the incident wavefront is important over the distance a, the present treatment becomes invalid.

IV. Effect of Curvature of the Incident Wavefront

(a) *Statement of Problem*

The previous approach based on Fourier analysis and the use of reciprocal space holds when the incident wave is effectively plane and the observations of the scattering are made at a large distance from the irregularities. However, neither of these conditions applies when a point source of waves is used to irradiate the scattering medium and the observations of the scattering are made at a point relatively close to the irregularities. Under these circumstances, the incident wavefront is curved and, in adding up the contributions to the scattering from different elements of the medium, the varying distances of the elements from the receiver have to be taken into account. Both factors introduce additional phase variations.

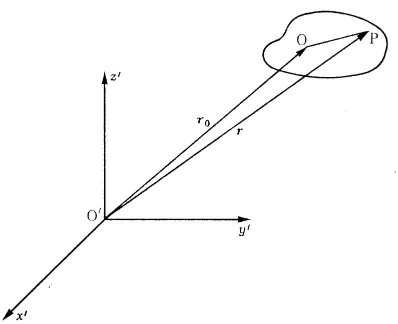

Fig. 4.—Coordinate system for numerical calculation of back-scattering when the finite distance of the irregularity from the transmitter and receiver is taken into account.

Consider a scattering region as in Figure 4, in which P is the location of a scattering element and O is the location of an arbitrary coordinate system (x, y, z). The position vectors of P and O relative to the observer's coordinate system of origin O′ and axes (x', y', z') are $\boldsymbol{r}$ and $\boldsymbol{r}_0$ respectively. The amplitude of the incident wave at P is proportional to $r^{-1}\exp(-ikr)$, where $k = 2\pi\lambda^{-1}$ and $r = |\boldsymbol{r}|$. Hence, if the scattering power per unit volume at P is $f(\boldsymbol{r}) = f(x, y, z)$, the power scattered from a volume element $\mathrm{d}V = \mathrm{d}x\,\mathrm{d}y\,\mathrm{d}z$ is

$$r^{-1}\exp(-ikr)\,f(\boldsymbol{r})\,\mathrm{d}V.$$

The scattered wave spreads out as a spherical wave and the back-scattered amplitude at a point close to the transmitter therefore contains the additional multiplying factor $r^{-1}\exp(-ikr)$. Thus the total returned amplitude may be written

$$\int_0^\infty\int_0^\infty\int_0^\infty r^{-2}\exp(-2ikr)\,f(\boldsymbol{r})\,\mathrm{d}V. \tag{13}$$

This expression contains no approximations apart from the omission of polarization considerations which are relevant in the case of electromagnetic waves but are not usually important unless the scattering angles are very large.

In order to see how the expression (13) is related to the plane wave approximation used in Section III, we first write the three-dimensional Fourier transform of $f(\boldsymbol{r})$ as

$$F(\mathbf{v}) = \int_0^\infty \int_0^\infty \int_0^\infty f(\boldsymbol{r}) \exp(2\pi \mathrm{i}\, \mathbf{v} \,.\, \boldsymbol{r})\, \mathrm{d}V, \tag{14}$$

where $\mathbf{v}$ is a position vector in reciprocal space and $F(\mathbf{v})$ is the density in reciprocal space at the point $\mathbf{v}$. On the plane wave approximation, the back-scattered amplitude

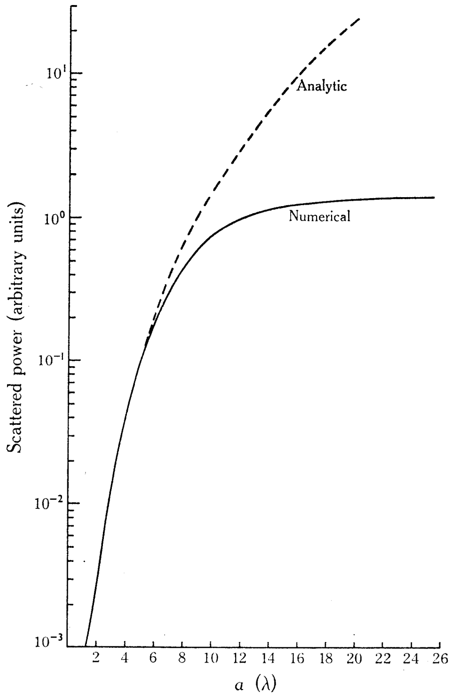

Fig. 5.—Comparison of (approximate) analytic calculation of back-scattered power with exact numerical computation for an irregularity of Gaussian form at a range of $600\,\lambda$ from the transmitter and receiver. The curves diverge for horizontal scales greater than $\sim 10\,\lambda$ because curvature of the wavefront then becomes important.

is proportional to the density in reciprocal space at a point $2\lambda^{-1}$ from the origin along a line measured in the reverse direction to the incident wave. This point is

$$\mathbf{v} = -2\lambda^{-1}\hat{\boldsymbol{r}}_0,$$

where $\hat{\boldsymbol{r}}_0$ is a unit vector in the direction of $\boldsymbol{r}_0$. Thus the back-scattered amplitude is proportional to

$$\int_0^\infty \int_0^\infty \int_0^\infty f(\boldsymbol{r}) \exp(-2\mathrm{i}k\,\hat{\boldsymbol{r}}_0 \,.\, \boldsymbol{r})\, \mathrm{d}V. \tag{15}$$

Now, if all elements of the scattering volume are at a large distance from the origin and the angle between $\boldsymbol{r}$ and $\boldsymbol{r}_0$ is small, the expression (13) can be evaluated approximately by taking the factor r^{-2} outside the integral and writing $r \approx \hat{\boldsymbol{r}}_0 \,.\, \boldsymbol{r}$ (the latter approximation is equivalent to the assumption that the phase at (x, y, z) is the same as that for a plane wave proceeding in the direction r_0). With these approximations the expressions (13) and (15) are equivalent. Although this clarifies the transition from the exact to the approximate formula, it does not indicate how serious the use of the approximation (15) is likely to be in a particular situation. In order to test this, we have carried out some numerical calculations.

(*b*) *Numerical Tests*

The integral (13) cannot usually be evaluated analytically and so we have evaluated it numerically by digital computer for some particular cases. An elliptical Gaussian irregularity was assumed and the density was specified at a number of equally spaced points over a three-dimensional lattice in (x, y, z) space. The integral (13) was evaluated numerically using a repetitive application of the trapezoidal rule which, for functions of the form $f(g)\exp(-g^2)$, allows the use of larger step intervals than other integration techniques. The integrations were repeated until successive halving of the step interval gave no significant difference between one step and the next and then the results were compared with the approximate theory. Results for typical circumstances ($b = 0{\cdot}2\,\lambda$ and a range of $600\,\lambda$) plotted in Figure 5 show that the exact and approximate theories agree up to values of a of the order of $10\,\lambda$. For larger values of a the actual scattering is considerably less than that given by the approximate theory.

V. Conclusions

The purpose of the paper has been to stress the importance of taking into account geometrical factors and polar diagrams of transmitters and receivers when making deductions from radar observations of atmospheric irregularities. If the irregularities are isotropic, these instrumental factors completely determine the results obtained and no information about the irregularities themselves can be derived. If the irregularities are anisotropic, with different horizontal and vertical dimensions, information about the horizontal scales may be obtained in some cases. The range of validity of the theory has been checked by means of numerical calculations of the scattering for one particular example.

VI. Acknowledgments

This work forms part of a program of observations of ionospheric irregularities supported by the Australian Research Grants Committee and the Radio Research Board. We are greatly indebted to Mr. A. C. Beresford for writing computer programs for the numerical calculations described in Section IV and for helpful discussions.

VII. References

Briggs, B. H. (1961).—*Proc. phys. Soc.* **77**, 305.

Gardner, F. F., and Pawsey, J. L. (1953).—*J. atmos. terr. Phys.* **3**, 321.

McAllister, L. G., Pollard, J. R., Mahoney, A. R., and Shaw, P. J. R. (1969).—*Proc. Instn elect. Engrs* **57**, 579.

Ratcliffe, J. A. (1956).—*Rep. Prog. Phys.* **19**, 188.

Vincent, R. A. (1973).—*Aust. J. Phys.* **26**, 815.